Transactions, SMiRT-23
Manchester, United Kingdom - August 10-14, 2015
Division X

ON THE CALCULATION OF DESIGN DEMANDS FOR ACCIDENT THERMAL LOADING COMBINATION

Saahastaranshu R. Bhardwaj[1], Amit H. Varma[2], Kadir C. Sener[3]

[1] Ph.D. student, Lyles School of Civil Engineering, Purdue University, West Lafayette, IN 47906, USA
[2] Professor, Lyles School of Civil Engineering, Purdue University, West Lafayette, IN, USA
[3] Research Engineer, Lyles School of Civil Engineering, Purdue University, West Lafayette, IN, USA

ABSTRACT

Reinforced concrete walls and slabs in safety-related nuclear facilities are required to be designed for abnormal load combinations. This paper evaluates the design force demands on safety-related nuclear structures due to accident thermal loads. Thermal loading conditions and effects of thermal loads and restraints on structural behavior are discussed. Idealized possible structure geometries for nuclear facilities are analyzed and the modeling and analysis parameters are briefly discussed. Selected structures are subject to LEFE and NIFE analysis for idealized accident thermal loads. The demands from LEFE and NIFE analysis are compared to predict the effectiveness of simple LEFE analysis. The demand to capacity ratio (DCR) for individual demands are also calculated. Additionally, the paper delves into the effectiveness of concrete clear cover in reducing the magnitude of stresses due to thermal loads.

The paper presents guidelines and recommendations to perform finite element analysis for safety-related nuclear facilities. Simplistic LEFE analysis is compared with a NIFE analysis to determine the conservatism of the LEFE analysis. Individual DCRs are calculated to highlight the design procedure for concrete walls and slabs. However, the interaction of demands is not considered in the paper. It needs to be addressed while designing the structures for various load combinations.

It is observed that the LEFE analysis can be used to conservatively predict the demands. LEFE analysis is recommended to be performed for temperature at the centroid of rebar closest to the edge of the wall.

INTRODUCTION

Safety-related nuclear facilities are labyrinthine in nature consisting of numerous walls and slabs that are made of reinforced concrete. For example, the entire containment internal structure (CIS) of a nuclear power plant consists of numerous interconnected concrete walls and slabs. These safety-related structures may be subjected to abnormal loads (accident thermal and pressure loads, P_a, T_a, R_a, Y_r, Y_j, and Y_m) generated by a postulated high-energy pipe break accident.

ACI 349 (ACI, 2006) specifies that structures and structural members shall have design strengths at least equal to the required strengths calculated for the factored load combinations stipulated in Section 9.2 of the code. These load combinations include factored combinations of normal, severe or extreme environmental, and abnormal loads. For example, Equation 1 below includes combination of normal loads (dead D, live L, flood F, hydraulic H, and operating thermal T_o and R_o) and extreme environmental loads (seismic E_{ss}). Equation 2 includes combination of normal loads (D, F, L, and H), extreme environmental loads (E_{ss}) and abnormal loads (P_a, T_a, R_a, Y_r, Y_j, and Y_m). Most loading combinations include either operating thermal (T_o), or accident thermal conditions (T_a).

$$U = D + F + 0.8L + C_{cr} + H + T_o + R_o + E_{ss} \quad \text{(Eq. 9-6 of ACI 349)} \quad (1)$$

$$U = \mathrm{D} + \mathrm{F} + 0.8\mathrm{L} + \mathrm{H} + (T_a + R_a + P_a) + (Y_r + Y_j + Y_m) + E_{ss} \quad \text{(Eq. 9-9 of ACI 349)} \quad (2)$$

The demands due to individual loads can be determined using linear elastic finite element (LEFE) analysis. The individual demands can then be superimposed to determine the demand for a particular load combination. An elaborate non-linear inelastic finite element (NIFE) analysis can also be performed to determine the individual demands.

This paper focuses on determination of demands due to accident thermal conditions. Thermal loading conditions and effects of thermal loads and restraints on structural behavior are discussed. Different idealized structure geometries for nuclear facilities are analyzed and the modeling and analysis parameters are briefly discussed. LEFE and NIFE analysis is performed for selected structures subjected to idealized accident thermal loads. The demands from LEFE and NIFE analysis are compared to establish the conservatism of simple LEFE analysis. LEFE analysis is performed for temperatures at three different locations on the rebar layers to ascertain the location that yields results similar to NIFE analysis. The demand to capacity ratios (DCRs) for individual force and moment demands are also calculated. Additionally, the paper delves into the effectiveness of concrete clear cover in reducing the magnitude of stresses due to thermal loads.

The paper presents guidelines and recommendations to perform finite element analysis for safety-related nuclear facilities. Simplified LEFE analysis is compared with a NIFE analysis to determine the conservatism of the LEFE analysis. Individual DCRs are calculated to highlight the design procedure for concrete walls and slabs. However, the interaction of demands is not considered in the paper. It needs to be addressed while designing the structures for various load combinations.

THERMAL LOADS

Operating thermal loads are produced as consequences of normal operation of the facility. They also include the thermal loads associated with changes in ambient and weather conditions for exposed surfaces of walls. Operating thermal loads develop over long duration of time (several days of operation), and consequently produce steady state temperatures with linear variation through the thickness of the concrete elements. The surface temperatures of the concrete elements are the same as the ambient air temperature within the respective compartment. No concrete cracking is associated with these steady state temperatures and linear variations through the thickness of the concrete element. Restraints to thermal deformations produce significant stresses and forces, which can be estimated by LEFE analysis of the structure and included as the calculated required strengths for operating thermal conditions.

Accident thermal loads are typically associated with postulated high-energy pipe break scenarios. Thermal-hydraulic analyses are conducted to simulate the effects of these high-energy pipe break events. The results include the temperature histories (*T-t* plots) for exposed surfaces of the concrete elements. These temperature histories (surface *T-t* plots) define the accident thermal loads (T_a) for structural analysis and design. Typical accident temperature-time histories for each major compartment in the CIS are identified using envelopes of T-t histories from publicly available design control documents by Sener et al. (2015).

For example, Figure 1 shows idealized but representative temperature histories (*T-t* curves) for the surfaces (exterior and interior) of a concrete compartment open at the top and subjected to high-energy pipe break event. As shown, both surfaces of the concrete walls have slightly different temperature histories, and the interior surface temperature leads the exterior surface temperature for a few hours. As shown in Figure 1, the surface temperature increases to 280-300^{o}F from the operating temperature (100-120^{o}F) over the first few (10-20) minutes of the event. The temperature reduces to 190-210^{o}F over the next day (24 hours), and then reduces slowly to 180^{o}F over the next ten days (240 hours). The specific details of the *T-t* curves will vary depending on the details of the compartment and the accident event.

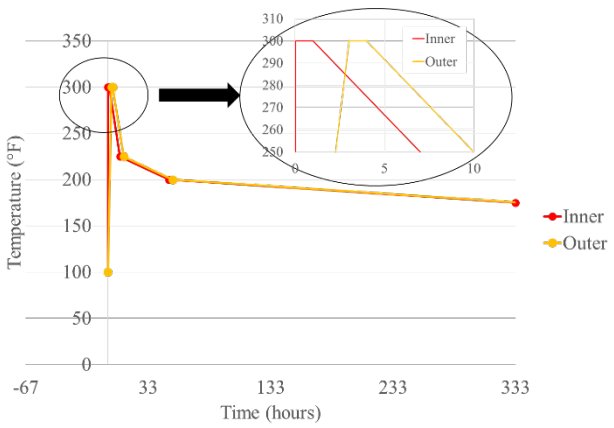

Figure 1. Temperature histories for Concrete Compartment Surfaces

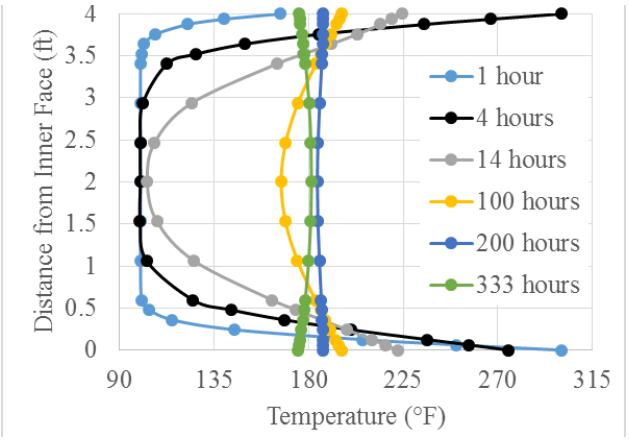

Figure 2. Temperature contours through the section at different time steps

The temperature histories (*T-t* curves) for various points through the thickness of the concrete wall, and the temperature profiles through the thickness of the concrete wall at different times are calculated by performing heat transfer analysis through the concrete cross-section without accounting for steel reinforcement. The heat transfer analysis can be performed using the finite difference method or the finite element method, while modeling the concrete thickness and the steel reinforcement and steel liner plates explicitly for more accuracy. Alternately, the heat transfer analysis can be performed using the one-dimensional heat conduction equation while modeling the concrete thickness alone without any steel. In this case, the steel temperatures are assumed equal to the concrete temperatures at the corresponding locations.

Figure 2 shows sample temperature profiles that were calculated through the thickness of 48 in. thick concrete wall subjected to the surface temperature histories (*T-t* curves) shown in Figure 1. The temperature histories (*T-t* curves) for points through the thickness can be calculated by performing heat transfer analysis using the one-dimensional heat conduction equation and concrete thermal and material properties. The thermal gradient through the wall thickness is significantly nonlinear for several hours (almost up to one day) after the event. The temperatures become relatively uniform through the thickness after several (three to four) days. The specific details of the thermal gradients and their evolution over time will depend on the details of the concrete wall and the surface temperature histories (*T-t* curves) generated by the accident event.

STRUCTURAL BEHAVIOR

Operating thermal loads produce linear thermal gradients through the thickness of the structural element. These temperature changes induce thermal deformations due to expansion (or contraction) of the concrete and steel materials in the structural member. If these thermal deformations are restrained by end conditions or connected members, restraining forces are induced in the structural elements. If these restraining forces are membrane tension, concrete will crack, relieve these forces and undergo the associated thermal deformation. If the restraining forces are membrane compression, they will be resisted by the concrete and steel together. If these restraining forces are membrane shear, out-of-plane shear, or out-of-plane flexure, there will be some concrete cracking, but the restraining forces will not be relieved. The restraining forces will depend on stiffness of the member subjected to thermal loads and the relative stiffness of the restraining member or structure, both of which are included in the structural analysis model used to estimate the required strengths associated with operating thermal loads.

The structural behavior of concrete members subjected to accident thermal loading can be complicated and varying over duration of the event. As discussed, during the first few hours (up to one day) of the accident, structural members are subjected to significantly nonlinear thermal gradients over the thickness. These nonlinear thermal gradients induce significant concrete cracking due to internal or self-restraint. This is illustrated in Figure 3, which shows the qualitative behavior of a reinforced concrete section subjected to nonlinear thermal gradient (ΔT). Thermal strains (ε_{th}) are calculated directly as the thermal expansion coefficient (α) multiplied by ΔT. As a result, thermal strains have the same nonlinearity as the thermal gradient. Since plane sections remain plane, total strains (ε_{tot}) vary linearly over the thickness, which produces internal or self-restraint. Mechanical strains (ε_{mech}) are equal to the total strains (ε_{tot}) minus the thermal strains (ε_{th}). As shown in Figure 3, significant portion of the member thickness is subjected tensile mechanical strains, which causes cracking of the concrete. The total strains (ε_{tot}), which depend on the centroidal strain (ε_{cen}) and curvature (ϕ), can be calculated by establishing force equilibrium over the cross-section. Thus, during the first few hours (up to one day) of the accident event, there is significant cracking through the thickness of the concrete member due to self-restraint.

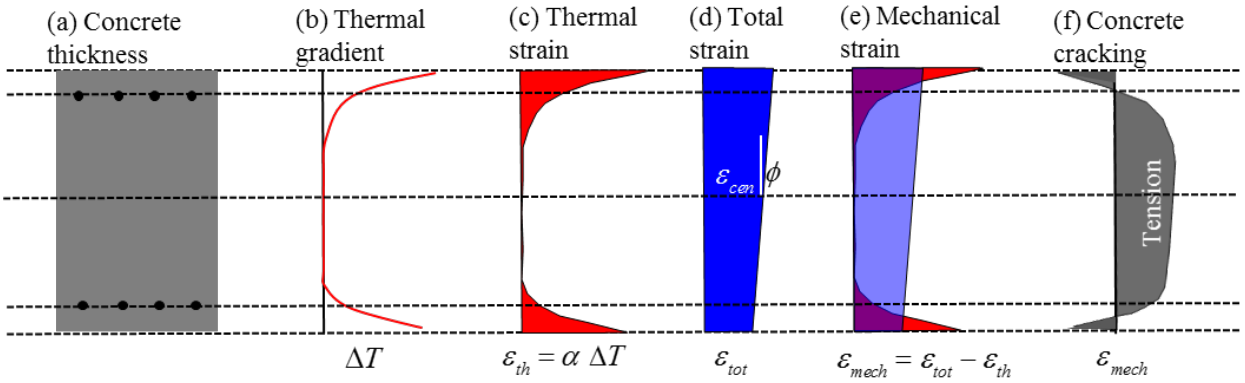

Figure 3. Concrete cracking due to nonlinear thermal gradient from accident event

After the first few hours (up to one day) of the accident, the thermal gradients become relatively uniform through the thickness as shown in Figure 2. The concrete cracks, produced during the first few hours due to self-restraint, close due to the uniformity of the temperatures through the thickness. The uniform temperatures are lower than the maximum values reached earlier. However, the concrete will never regain its uncracked stiffness for mechanical loads. In the rare situation of the thermal expansion being fully restrained, there will be no concrete cracking, even for the case with nonlinear thermal gradients. The membrane axial compression associated with full restraint will be equal to the integration of the thermal stresses ($E\ \varepsilon_{th}$) over the member area.

STRUCTURE GEOMETRY AND MODEL PARAMETERS

The structures in safety-related nuclear facilities have different geometries. In order to cover a range of geometries, three idealized geometric shapes are considered for this analysis. These are i) rectangular in plan (Rectangle), ii) circular in plan, e.g. reactor water storage pit (Circle) and iii) polygonal in plan, e.g. steam generator (Polygon) tank. For the purpose of analysis only the tank walls have been modeled with fixed boundary condition at bottom and free boundary condition at top. The details of the structures are presented in Figure 4. The structures are subject to accident thermal load presented in Figure 1. The thickness of the walls has been kept constant at 48 in. for all the geometries. Two layers of #11 bars @ 12 in. are placed on each face in vertical and horizontal directions for all the geometries. Additional analysis were performed with one layer of reinforcement spaced at 6 in. However, the thermal demands were found similar to the demands for sections with two layers of reinforcement. For brevity, the cases with single layer are not presented in this paper. Two legged #5 tie hoops @ 12 in. are used as shear reinforcement. In order

to understand the effect of concrete cover on accident thermal demands, four concrete clear covers, c_c, (0.75 in., 1.5 in., 2 in., 3 in.) are considered.

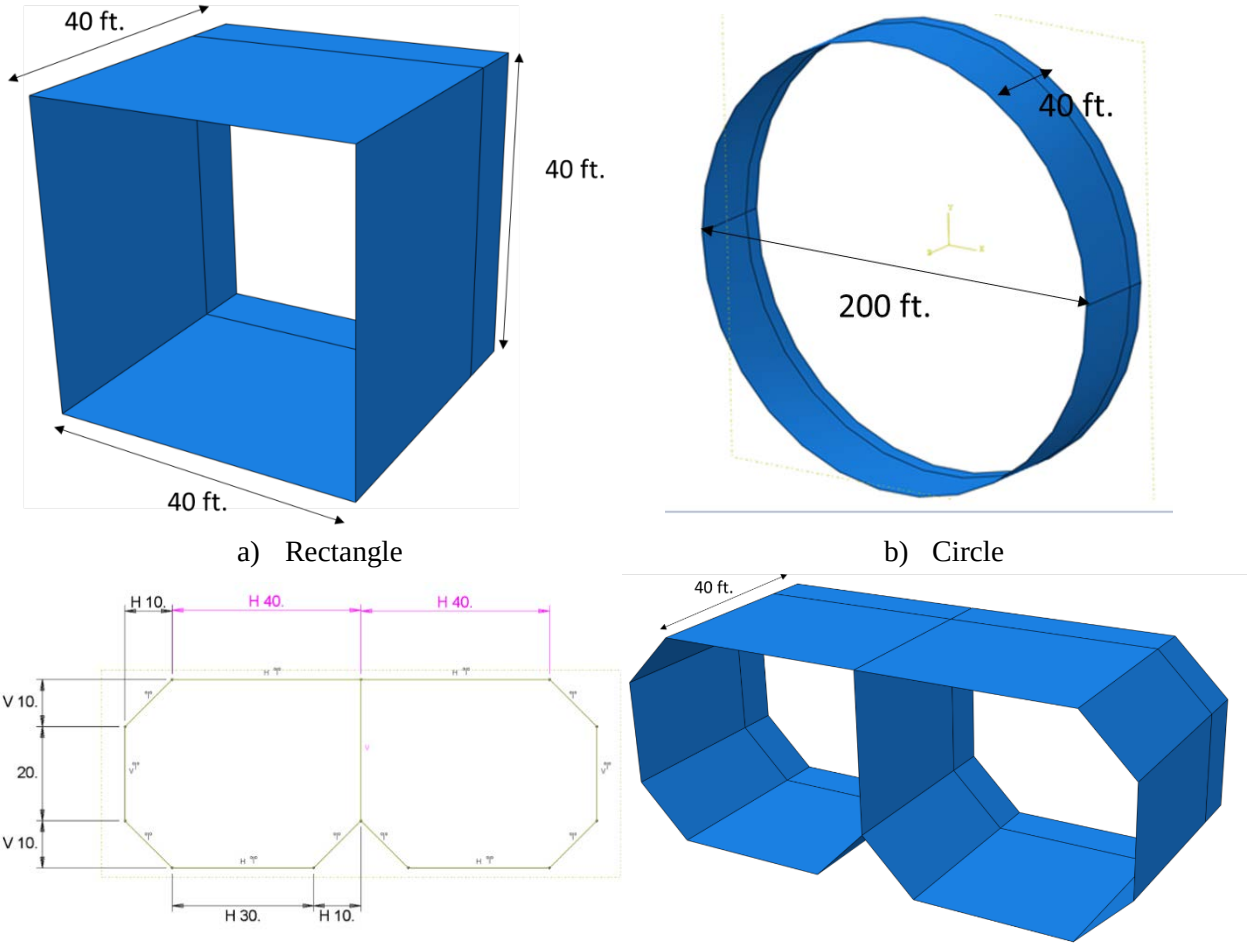

a) Rectangle

b) Circle

c) Plan view of Polygon geometry

d) Polygon

Figure 4. Geometries considered for analysis

ANALYSIS TYPES AND MODEL PARAMETERS

NIFE Analysis

Sequentially coupled thermal-stress NIFE analysis of the three geometries is performed using commercially available software ABAQUS (Dassault, 2013). In this method the heat transfer analysis of the structure is performed and the results of the analyses are used as input for the explicit dynamic stress analysis of the structures. For the heat-transfer analysis, the time-temperature data for inner and outer walls is applied as loading (boundary) conditions. The nodal temperatures at regular time intervals are calculated and output using the thermal properties of materials. The nodal temperatures from the heat transfer analysis are specified as the input (loading) for the structural analysis. Layered composite shell (LCS) elements are used for the analyses. The LCS elements can account for: (i) full composite action between the steel reinforcement and concrete infill, (ii) concrete cracking, (iii) steel reinforcement yielding. Nine concrete layers have been used to model the cross-section thickness. The reinforcement is embedded in the layers corresponding to the location of the bars. Shear reinforcement is not modelled in the analysis. The element

type used for heat transfer analysis is the 4-node quadrilateral heat transfer shell element (DS4). For structural analysis 4-node reduced integration, hourglass control, finite membrane strain shell elements have been used (S4R).

Since the thermal-stress analysis is sequentially coupled, separate heat transfer and structural analysis models for each structure have been built. The thermal properties have been taken from Hong & Varma (2009). For stress models, the thermal expansion coefficients for both steel and concrete have been taken from Eurocode 4 (EN 1994-1-2, 2005). The steel modulus of elasticity has also been taken from Eurocode 4. However concrete modulus of elasticity has been obtained using provisions of Section 8.5 of ACI 349 (ACI, 2006). The concrete material model uses a plasticity based approach with concrete damaged plasticity (CDP) model in ABAQUS. The concrete models are defined with the following parameters: elastic modulus, Poisson's ratio, uniaxial stress-strain behavior in compression, uniaxial stress-strain behavior in tension, and mass density. The uniaxial compression stress-strain behavior of concrete was defined using the modified Popovic's empirical stress-strain model recommended by Collins et al. (1993). The uniaxial tension strength and the post-peak behavior are defined using the equations for plain concrete provided in CEB-FIP Model Code (CEB, 1990). The concrete compressive strength is taken equal to 4-ksi. Reinforcement has been modelled as elastic perfectly plastic with a yield stress of 60-ksi.

Two mesh sizes are used in the models. The mesh size is based on the section thickness, 't_{sc}'. The bottom $2t_{sc}$ high region of the structures uses mesh size of $t_{sc}/4 \times t_{sc}/2$. The top region uses $t_{sc} \times t_{sc}/2$. The stress variation is greater near the restraint (bottom). A finer mesh at bottom ensures that these variations are better captured. Figure 5 illustrates the mesh used for Rectangle tank analyses. Similar mesh size is used for Circle and Polygon.

LEFE Analysis

The LEFE analysis does not account explicitly for the effects of: (i) concrete cracking, (ii) nonlinear thermal gradients and temperature profiles through the cross-section. It consists of using a linear elastic model that implicitly accounts for the effects of concrete cracking by using reduced stiffness values. For LEFE analysis, the elastic modulus (E_m) and poisson's ratio (ν_m) of the material, and the thickness (t_m) of the element are edited to model the cracked flexural, axial, and shear stiffness of the concrete member. The flexural, axial, and shear stiffness of concrete members are based on the effective stiffness values for cracked members in Table 6-5 of ASCE 41-13 (ASCE, 2013). The model equivalent cracked elastic modulus value (E_m) obtained is 4617 ksi and the model thickness (t_m) is 35.1 in. The model Poisson's ratio is that for concrete (ν_m=0.17). The analysis is single step with the initial temperature set at the operating temperature (100°F) and the final temperature being the maximum temperature rise in chosen section location. The analysis is performed by considering the temperatures at three possible locations (C, T and G) as shown in Figure 6, where c_c is the clear concrete cover, t_c is the thickness of the wall. Location C is the edge of the clear cover, T is the centroid of rebar closest to the edge and G is the centroid of the rebar group.

Homogeneous elastic shell elements are used for the analysis. The element type used is S4R (4-node doubly curved thin or thick shell, reduced integration, hourglass control, finite membrane strains). Layered composite shells are not required because a constant temperature is applied to an equivalent elastic material model. The mesh size used for NIFE models has also been used for the LEFE models. This is to ensure ease of comparison of results from LEFE and NIFE models. The mesh size for LEFE models is also based on the actual section thicknesses

DEMAND CAPACITY RATIO (DCR) CALCULATION

The available strength of the walls for individual demand types can be determined using the provisions of ACI 349. The membrane axial compression strength per unit width (12 in), P_n, is given by Equation 3 below (Equation 10-2 of ACI 349). The in-plane shear strength per unit width (12 in), V_{ni}, is given by Equation 4 (ACI 349 Section 21.7.4.4). The out-of-plane shear strength per unit width (12 in), V_{no}, is given by Equation 5, where V_c is the concrete contribution and V_s is the contribution of shear reinforcement. Concrete contribution, V_c is given by Equation 6 (ACI 349 Section 11.3.1.1). Steel contribution, V_s, is given by Equation 7 (ACI 349 Section 11.5.7.2). The out-of-plane moment capacity is determined considering the unit width of the wall as a beam with compression reinforcement. In these equations, f'_c is the concrete compressive strength, f_y is the steel yield strength, A_g is the gross cross-section area, A_c is the cross-section area of concrete, A_{st} is the cross-section area of the steel reinforcement, A_v is the cross-section area of shear reinforcement, f_{yt} is the shear reinforcement yield strength, s is the spacing of shear reinforcement and d is the distance of extreme compression fiber from the centroid of tension reinforcement (conservatively taken as 44 in. for all analysis).

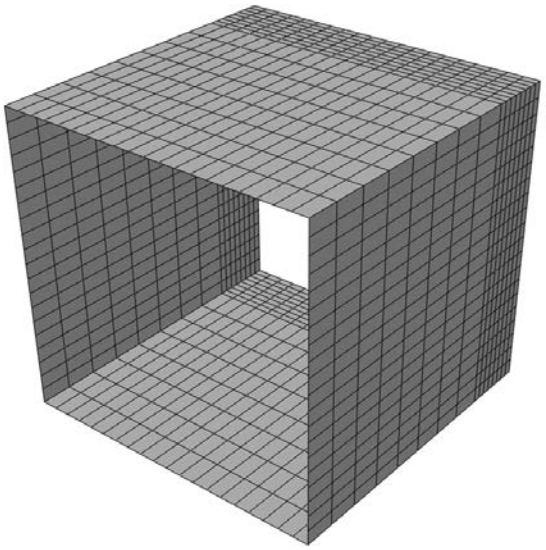

Figure 5. Finite Element Mesh for Rectangle

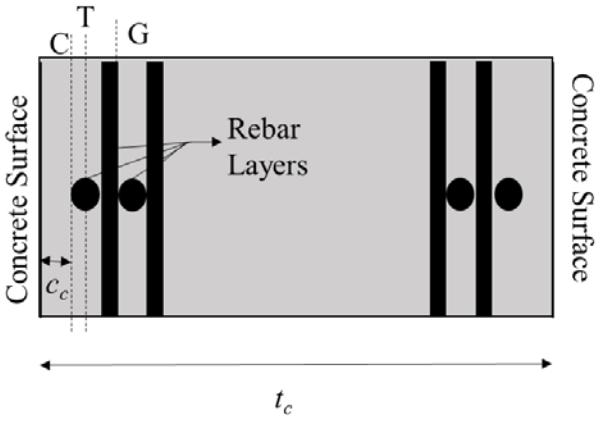

Figure 6. Wall Section showing locations where temperature is considered for LEFE analysis

$$P_n = 0.8\left[0.85 f_c^{'}(A_g - A_{st}) + f_y A_{st}\right] \quad (3)$$

$$V_{ni} = 10\sqrt{f_c^{'}}\,(A_c) \quad (4)$$

$$V_{no} = V_c + V_s \quad (5)$$

$$V_c = 2\sqrt{f_c^{'}}\,(A_c) \quad (6)$$

$$V_s = \frac{A_v f_{yt} d}{s} \quad (7)$$

Table 1 presents the peak temperatures at the three locations shown in Figure 6 (C, T and G) for the accident thermal loading. The temperatures are obtained from the thermal analysis performed as a part of NIFE analysis. These can also be obtained by performing a 1-D heat conduction analysis using finite difference method. Since the thickness and accident thermal load is the same for the three geometries, the through thickness temperature profile is the same for all. It is observed that the peak temperature at the rebar location

reduces as the clear cover increases. Additionally, the temperature drops significantly as the location of measurement (C, T and G) moves away from the surface.

Table 1. Peak Temperature at C, T and G locations

Concrete Clear Cover (in.)		0.75	1.50	2.00	3.00
Temperature (°F)	at C	267	243	231	211
	at T	244	226	216	200
	at G	202	192	188	187

LEFE analysis is performed considering temperatures at the three locations from Table 1. The required strengths for individual demand types are obtained from LEFE analysis for all the cases. NIFE analysis is performed using the idealized time-temperature curves given in Figure 1 for all three geometries with four different concrete clear cover thicknesses. The maximum force and moment demands from NIFE analysis are observed near the base of the structures at 200 hours of heating. The required strengths are compared with available strengths discussed above and DCR values are determined. Figure 7 presents the DCR values for Rectangle for LEFE and NIFE analysis for different values of clear cover, c_c. The LEFE DCRs are determined for different concrete clear cover cases considering temperatures at C, T and F locations. The LEFE DCR values are color coded based on how they compare with the value for NIFE analysis. The LEFE DCRs that are greater than the NIFE DCRs are colored blue. Otherwise, the LEFE DCRs are colored red. Similarly, Figures 8 and 9 present the DCR values for Circle and Polygon respectively.

Demand Type	NIFE	LEFE C	LEFE T	LEFE G
Axial (SF1)	0.337	0.887	0.755	0.524
In-Plane Shear (SF3)	0.213	0.805	0.686	0.475
Out-of-Plane Shear (SF5)	0.580	0.790	0.673	0.467
Hoop Moment (SM1)	0.600	0.207	0.177	0.122
Vertical Moment (SM2)	0.697	1.032	0.879	0.609

a) c_c =0.75 in.

Demand Type	NIFE	LEFE C	LEFE T	LEFE G
Axial (SF1)	0.352	0.749	0.654	0.471
In-Plane Shear (SF3)	0.210	0.681	0.594	0.428
Out-of-Plane Shear (SF5)	0.521	0.668	0.583	0.420
Hoop Moment (SM1)	0.625	0.179	0.156	0.113
Vertical Moment (SM2)	0.683	0.891	0.777	0.560

b) c_c =1.5 in.

Demand Type	NIFE	LEFE C	LEFE T	LEFE G
Axial (SF1)	0.354	0.682	0.598	0.451
In-Plane Shear (SF3)	0.206	0.619	0.543	0.409
Out-of-Plane Shear (SF5)	0.526	0.607	0.533	0.402
Hoop Moment (SM1)	0.643	0.166	0.145	0.110
Vertical Moment (SM2)	0.664	0.825	0.724	0.545

c) c_c =2 in.

Demand Type	NIFE	LEFE C	LEFE T	LEFE G
Axial (SF1)	0.354	0.570	0.513	0.445
In-Plane Shear (SF3)	0.202	0.518	0.466	0.404
Out-of-Plane Shear (SF5)	0.506	0.508	0.457	0.397
Hoop Moment (SM1)	0.637	0.142	0.128	0.111
Vertical Moment (SM2)	0.621	0.709	0.637	0.553

d) c_c =3 in.

Figure 7. Comparison of DCR for Rectangle

Demand Type	NIFE	LEFE C	LEFE T	LEFE G
Axial (SF1)	0.439	0.948	0.807	0.560
Out-of-Plane Shear (SF5)	0.414	0.862	0.734	0.508
Hoop Moment (SM1)	0.627	0.328	0.280	0.194
Vertical Moment (SM2)	0.982	1.933	1.644	1.140

a) c_c =0.75 in.

Demand Type	NIFE	LEFE C	LEFE T	LEFE G
Axial (SF1)	0.423	0.801	0.699	0.504
Out-of-Plane Shear (SF5)	0.391	0.728	0.635	0.458
Hoop Moment (SM1)	0.644	0.284	0.247	0.178
Vertical Moment (SM2)	0.971	1.668	1.454	1.049

b) c_c =1.5 in.

Demand Type	NIFE	LEFE C	LEFE T	LEFE G
Axial (SF1)	0.416	0.729	0.640	0.482
Out-of-Plane Shear (SF5)	0.392	0.662	0.581	0.438
Hoop Moment (SM1)	0.652	0.263	0.230	0.173
Vertical Moment (SM2)	0.971	1.544	1.355	1.020

c) c_c =2 in.

Demand Type	NIFE	LEFE C	LEFE T	LEFE G
Axial (SF1)	0.407	0.610	0.549	0.476
Out-of-Plane Shear (SF5)	0.378	0.554	0.498	0.433
Hoop Moment (SM1)	0.674	0.226	0.203	0.176
Vertical Moment (SM2)	0.957	1.327	1.193	1.035

d) c_c =3 in.

Figure 8. Comparison of DCR for Circle

Demand Type	NIFE	LEFE C	LEFE T	LEFE G
Axial (SF1)	0.419	0.939	0.799	0.554
In-Plane Shear (SF3)	0.256	0.969	0.825	0.572
Out-of-Plane Shear (SF5)	0.782	1.316	1.121	0.777
Hoop Moment (SM1)	0.654	0.470	0.400	0.277
Vertical Moment (SM2)	1.103	1.989	1.694	1.174

a) c_c =0.75 in.

Demand Type	NIFE	LEFE C	LEFE T	LEFE G
Axial (SF1)	0.402	0.793	0.692	0.499
In-Plane Shear (SF3)	0.246	0.818	0.714	0.515
Out-of-Plane Shear (SF5)	0.756	1.112	0.971	0.700
Hoop Moment (SM1)	0.666	0.406	0.354	0.255
Vertical Moment (SM2)	1.079	1.718	1.498	1.080

b) c_c =1.5 in.

Demand Type	NIFE	LEFE C	LEFE T	LEFE G
Axial (SF1)	0.393	0.722	0.633	0.477
In-Plane Shear (SF3)	0.258	0.744	0.653	0.492
Out-of-Plane Shear (SF5)	0.765	1.012	0.888	0.669
Hoop Moment (SM1)	0.689	0.375	0.329	0.248
Vertical Moment (SM2)	1.074	1.590	1.395	1.051

c) c_c =2 in.

Demand Type	NIFE	LEFE C	LEFE T	LEFE G
Axial (SF1)	0.385	0.604	0.543	0.471
In-Plane Shear (SF3)	0.246	0.623	0.560	0.486
Out-of-Plane Shear (SF5)	0.720	0.847	0.762	0.661
Hoop Moment (SM1)	0.714	0.323	0.290	0.252
Vertical Moment (SM2)	1.067	1.366	1.228	1.066

d) c_c =3 in.

Figure 9. Comparison of DCR for Polygon

OBSERVATIONS

The observations from Figures 7, 8 and 9 are presented below.

i) The LEFE DCRs for hoop moment are consistently lower than the NIFE DCRs. This means that the LEFE model is unconservative with respect to hoop moment demands (values are colored red). The reason for lower hoop moment demands in LEFE analyses seems to be the underestimation of flexural stiffness used in hoop direction. The stiffness has been calibrated to cracked-transformed stiffness based on ASCE 41-13 recommendations. However, the compression due to the restraint near the base of the structures will cause the concrete to remain uncracked and thus increase the flexural stiffness and in turn the hoop moment demands.

ii) The LEFE analysis is conservative for all demand types (except hoop moment demands) for temperatures at locations C (edge of clear cover) and T (centroid of the rebar closest to the edge) (with the exception of one value for Rectangle). However, considering temperature at C will lead to higher demands and will be over-conservative. Therefore it is recommended that for LEFE analysis, temperature at the centroid of the rebar closest to the edge (T) should be considered.

iii) It is observed that the clear cover thickness does not affect the temperature distribution in the NIFE models. This is because the specific heat of steel is low as compared to concrete (though rebars were not included in thermal analysis, their inclusion will not change the results considerably). However, the LEFE temperature inputs are affected by the concrete clear cover. This is because the LEFE analysis is based on the rebar temperatures and greater covers reduce the rebar temperature.

iv) The concrete clear cover thickness does not have a significant influence on the NIFE DCRs. This is because the demands are maximized at 200 hours of heating, where the temperature distribution through the section is nearly uniform regardless of the concrete clear cover.

v) The LEFE DCRs are comparable with NIFE DCR's for concrete cover values of 2 in. and 3 in. These cover values are typical for reinforced concrete structures in safety-related nuclear facilities.

vi) The polygonal geometry indicates larger force and moment demands compared to the Rectangle and Circle geometries considered in the analysis. Since the Circle is an axisymmetric structure, the in-plane shear demands do not exist and have not been presented.

CONCLUSIONS

It is possible to conduct an elaborate nonlinear analysis of accident thermal conditions considering transient behavior and concrete cracking. However, such analyses require specialized expertise in modeling concrete cracking and conducting nonlinear analysis susceptible to convergence issues. Linear elastic analysis can be employed to obtain conservatively similar required strength values. LEFE analysis is recommended to be performed for temperature at the centroid of rebar closest to the edge of the wall.

FUTURE WORK

Steel-plate composite (SC) walls are increasingly being used in construction of safety-related nuclear facilities. The effectiveness of using a simplified LEFE analysis to obtain accident thermal demands for SC walls is currently being studied by the authors.

REFERENCES

ACI (2006). "Code Requirements for Nuclear Safety-Related Concrete Structures and Commentary", *ACI 349-06*, American Concrete Institute, Farmington Hills, MI.

ASCE (2013). "Seismic Evaluation and Retrofit of Existing Buildings", *ASCE/SEI 41-13*, American Society of Civil Engineers, Reston, VA.

CEB (1990). "CEB-FIP Model Code 1990". *Comité Euro-International du Béton*, EPF Lausanne, Case Postale 88, CH 1015, Lausanne, Switzerland.

Collins, M.P., Mitchell, D., MacGregor, J.G. (1993). "Structural Design Considerations for High Strength Concrete". *Concrete International: Design and Construction*, 15(5), pp 27-34.

Dassault (2013). "ABAQUS Analysis User's Manual", *Dassault Systèmes Simulia Corp*., Providence, RI, USA.

EN 1994-1-2 (2005). "Design of Composite Steel and Concrete Structures- Part 1-2: General Rules – Structural Fire Design", *Eurocode 4*. Eurpoean Committee for Standardization, Brussels, Belgium.

Hong, S., and Varma, A.H. (2009). "Analytical Modeling of the Standard Fire Behavior of Loaded CFT Columns," *Journal of Constructional Steel Research*, Volume 65, pp. 54-69, Elsevier.

Sener, K.C., Varma, A.H., and Bhardwaj, S.R. (2015). "Accident Thermal Loading Effects on Seismic Behaviour of Safety-Related Nuclear Structures." *Trans of SMiRT 23*, IASMiRT